Signal-Processing-Aided Distributed Compression in Virtual MIMO-Based Wireless Sensor Networks

Sudharman K. Jayaweera, *Member, IEEE*, Madhavi L. Chebolu, and Rakesh K. Donapati

***Abstract*—An adaptive signal-processing-aided distributed source coding scheme for virtual multiple-input–multiple-output communication-based wireless sensor networks (WSNs) is proposed. A computationally inexpensive distributed compression scheme that exploits the spatiotemporal correlations of sensor data is implemented with the aid of a recursive least squares (RLS)-based adaptive correlation tracking algorithm. The tracked correlation is used to compute side information that assists in distributed source compression. The proposed virtual space–time block coding and RLS-based compression side information are shown to improve energy efficiency at distributed nodes compared to previously proposed schemes with single-input–single-output communication. A semi-analytical approach is developed for energy efficiency analysis over different channel conditions and transmission distances. The energy efficiency performance of the proposed design is evaluated on real WSN data. The results show that the proposed integrated system outperforms conventional designs beyond certain transmission distance thresholds and leads to lower decoding errors, which makes it a good candidate for energy-aware WSNs.**

***Index Terms*—Adaptive signal processing, distributed compression, energy efficiency, virtual multiple-input–multiple-output (V-MIMO), wireless sensor networks (WSNs).**

I. Introduction

A TYPICAL wireless sensor network (WSN) consists of a set of spatially distributed sensor nodes that is wirelessly connected to a data-gathering node (DGN). Usually, the distributed nodes are battery operated. In many applications, their replacement can be expensive and/or difficult [1], which makes energy efficiency of paramount importance in designing large-scale, low-cost, and reliable sensor networks.

Naturally, one way to conserve node energy is to compress sensed data before transmission to the DGN. Of course, there are other possible information processing techniques that reduce energy consumption at network nodes. Some of these alternatives that have been explored in recent years include, for example, packet/data aggregation, energy-aware medium-access control protocols, and energy-efficient routing protocols [2]. The data compression in a distributed sensor network, however, can be challenging if intersensor communication among data collection nodes is to be avoided (or minimized). A compression scheme that exploits spatiotemporal data correlations while completely avoiding intersensor communication was proposed in [3]. Building on this basic compression algorithm, in this paper, we first develop a scheme that achieves better compression rates via better correlation tracking and data modeling.

An alternative approach for node energy conservation in any communication system is to reduce the per-bit-energy required for communication between the transmitter and the receiver. In a WSN, any improvement on this front can be a significant gain since, in most situations, the transmission energy is the dominant power consumption term. A promising solution that has gained wide applicability in cellular and wireless local-area networks (WLAN) and that provides previously unimaginable data rates and reliable transmission performance in the presence of channel fading is the multiple-input–multiple-output (MIMO) technique based on dual antenna arrays [4]–[8]. Different MIMO techniques such as space–time block coding (STBC) [9], [10], space–time trellis coding [11], and layered space–time designs [12] have been extensively studied for wireless cellular and WLAN systems during the past decade. However, MIMO techniques often require complex transceiver circuitry, sophisticated signal processing, and large physical dimensions to accommodate multiple antennas. Since the nodes in low-power WSNs are usually subjected to constraints on energy and physical dimensions, direct application of such MIMO techniques to wireless sensor systems does not seem realistic. The recently proposed virtual MIMO (V-MIMO) concept, however, allows the realization of MIMO techniques in a network of distributed nodes, each having only a single antenna, via node cooperation and the so-called local communications among nodes [13], [14]. In this paper, we integrate the above side-information-aided distributed compression scheme with the V-MIMO communication architecture of Cui *et al.* [13] and Jayaweera [14] that is based on distributed STBC. As we will note later, the proposed V-MIMO scheme necessarily requires data exchange among sensor nodes. However, an efficient integrated design is achieved by performing this exchange only on compressed data and limiting it to only the closest nodes. Note that the distributed STBC scheme of Cui *et al.* [13] and Jayaweera [14] is just one example of node cooperation

Manuscript received May 25, 2005; revised July 8, 2006 and November 30, 2006. This work was supported in part by the Kansas NASA EPSCoR program under Grant KUCR FED33144/KAN33145 and by the Kansas National Science Foundation (NSF) EPSCOR program under Grant KUCR NSF32195/KAN32196. The review of this paper was coordinated by Dr. M. Valenti.

S. K. Jayaweera was with the Department of Electrical and Computer Engineering, Wichita State University, Wichita, KS 67260 USA. He is now with the Department of Electrical and Computer Engineering, University of New Mexico, Albuquerque, NM 87131 USA (e-mail: jayaweera@ece.unm.edu).

M. L. Chebolu was with the Department of Electrical Engineering, Wichita State University, Wichita, KS 67260 USA. She is now with AT&T Bell Labs, Middletown, NJ 07748 USA.

R. K. Donapati was with the Department of Electrical Engineering, Wichita State University, Wichita, KS 67260 USA. He is now with Aeroflex Test Solutions, Wichita, KS 67215-8935 USA.

Color versions of one or more of the figures in this paper are available online at http://ieeexplore.ieee.org.

Digital Object Identifier 10.1109/TVT.2007.900361

in WSNs. In general, there is a significant amount of work on node cooperation and cooperative diversity in wireless networks [15]–[23]. Various forms of distributed space–time coding approaches have also been studied previously in [24] and [25]. A joint source–channel coding approach based on node cooperation in an additive white Gaussian noise (AWGN) channel, which can be viewed as a special case of the proposed V-MIMO scheme for fading channels, has previously been proposed in [26]. While a multiple-relay channel with a single source and a destination is strictly different from cooperative wireless networks, the two problems are of course somewhat related. The information-theoretic aspects of wireless networks with multiple relaying have recently been investigated, among others, in [27]–[29].

The remainder of this paper is organized as follows. In Section II, we describe our sensor network model and the integrated system design with V-MIMO communication and signal processing-aided distributed compression. In Section III, we present the proposed recursive least squares (RLS)-based correlation-tracking algorithm and an efficient encoding side-information computation method based on proper data modeling. In Section IV, we develop a semi-analytic approach to evaluate the energy consumption of the integrated system that takes into account both transmission and circuit power consumption in nodes. In Section V, we provide performance results of the proposed integrated design based on real WSN data. Finally, Section VI concludes this paper by discussing possible extensions.

II. Proposed Integrated System Description

We consider a typical WSN model in which a collection of low-end (limited-energy) sensor nodes are wirelessly connected to a high-end DGN that has no energy constraints. The distributed low-end sensors observe a physical phenomenon of interest and collect periodic data samples. The sensor nodes represent their observations using n-bits. Since node observations correspond to a common physical process, naturally, they are expected to be both spatially and temporally correlated.

The energy consumption in low-end nodes can be reduced by compressing n-bit observations by exploiting redundancy due to these inherent spatiotemporal correlations. Of course, one would like to perform this compression without any intersensor communications. The theoretical foundation for distributed compression that avoids intersensor communication is provided by the Slepian–Wolf theorem [30]. In the proposed design, we make use of an algorithm for distributed source compression with side information proposed in [3] to avoid intersensor communication. According to this scheme, all sensor nodes agree on a common tree-structured codebook that is also known to the DGN. The root node of the code tree is assigned all possible data points (2^n sample points). Next, the tree is developed by assigning data points of a parent node alternatively to its two children nodes. Thus, the code tree will have n-levels. The tree branches are labeled with 0 or 1 depending on whether its direction is to the left or to the right of a parent node, respectively. Here, we omit further details of codebook construction and refer the interested readers to [3].

Note that, according to this construction, the ith level of the tree consists of 2^i nodes, and each of these nodes can be given a unique label using only $i \leq n$ bits. In fact, the i bits corresponding to the branch labels from the root node to a given node provide such a unique label. Each node at the ith level, however, represents 2^{n-i} number of sample points that is called a subcodebook. Once correctly informed to which subcodebook an observed data point corresponds at the ith tree level, there is a way for the DGN to pick the true data point out of these 2^{n-i} possible choices in a particular subcodebook; then, it is enough for each node to send only those i-bit node labels to the DGN. This is precisely what our assumed distributed source compression scheme from [3] does. The value of i to be used is the encoding side information provided by the DGN to each node. Formally, let us denote the observation of sensor j at time k by $X_k^{(j)}$ and the encoding side information provided by the DGN to node j at time k by $i(k,j)$. The source encoding operation at node j first computes $f(X_k^{(j)}) =$ index $(X_k^{(j)}) \bmod 2^{i(k,j)}$. The $i(k,j)$-bit binary representation of $f(X_k^{(j)})$ is the bit stream that specifies the path from the root codebook to the subcodebook $\mathcal{S}$ at level $i(k,j)$ that contains the data point $X_k^{(j)}$. The compressed data that node j transmits at time k are thus the $i(k,j)$-bit binary representation of $f(X_k^{(j)})$.

Clearly, the above distributed source encoding scheme does not require node j to know anything about the observations of other nodes. Hence, it completely avoids intersensor communication. The only thing the node j needs is the encoding side information $i(k,j)$. In essence, the value $i(k,j)$ summarizes the correlation structure between $X_k^{(j)}$ and other nodes. However, it is computed by the DGN that tracks the data correlation structure, and fed back to the distributed nodes. Consequently, low-end nodes can blindly encode their observations, which leads to lightweight encoders.

Assuming that the $i(k,j)$ bit stream from node j representing $f(X_k^{(j)})$ is received at the DGN correctly, the first step in decompression process is to use this bit sequence to trace to the subcodebook $\mathcal{S}$ at the $i(k,j)$th level. Next, the observation $X_k^{(j)}$ is decoded as $\hat{X}_k^{(j)} = \arg\min_{r_m \in \mathcal{S}} \|Y_k^{(j)} - r_m\|$, where $\hat{X}_k^{(j)}$ is the decoded reading, $Y_k^{(j)}$ is the prediction of $X_k^{(j)}$ at the DGN, $\mathcal{S}$ is the subcodebook to which the actual reading $X_k^{(j)}$ belongs to, and r_m is the mth codeword in the subcodebook $\mathcal{S}$ for $m = 1, \ldots, 2^{n-i(k,j)}$. It was shown in [3] that if the difference between $X_k^{(j)}$ and its prediction $Y_k^{(j)}$ at the DGN is less than $2^{i(k,j)-1}\Delta$, where Δ is the quantization step of the analog-to-digital converter (ADC), then the reconstruction $\hat{X}_k^{(j)}$ will be perfect, and decoding errors will be avoided. For this reason, $2^{i(k,j)-1}\Delta$ is defined as the tolerable prediction noise level.

As will be explained in Section III, in this paper, we employ an RLS-based adaptive spatiotemporal prediction filter to generate prediction $Y_k^{(j)}$ at the DGN. The prediction error $e_k^{(j)} = Y_k^{(j)} - X_k^{(j)}$ is modeled as a zero-mean Gaussian random variable. This model is used to compute the encoding side information $i(k,j)$ that is fed back to the distributed nodes, as shown in Section III.

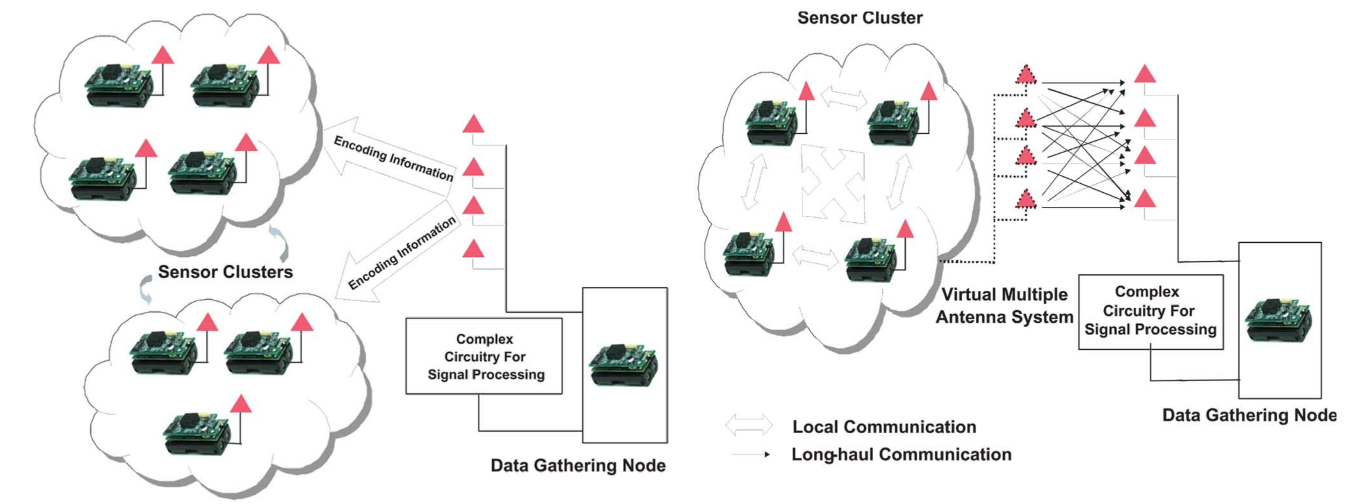

(a) (b)

Fig. 1. (a) Sensor cluster formation and encoding information transmission by the DGN. (b) Local and long-haul communications.

In the proposed integrated design, V-MIMO communication is used to transfer the compressed bits from each node [i.e., the binary representation of $f(X_k^{(j)})$] to the DGN. The V-MIMO technique proposed in [13] and [31] exploits node cooperation to overcome the problem of having a single antenna at each node. Note that while there have been several V-MIMO proposals for sensor networks in recent years [13], [14], [26], [32], in this paper, we confine ourselves to distributed STBC [9] with M-ary quadratic-amplitude modulation (QAM).

In V-MIMO, a set of nodes close to each other forms a cluster as in Fig. 1(a). Each node in the network associates itself with at least one predetermined cluster. Note that the distance between nodes in a cluster is assumed to be considerably less than the distance between a cluster and the DGN. Virtual space–time block encoding is performed in a cluster as if cluster nodes were elements of an antenna array. This requires all cluster nodes to have the same input data sequence necessitating intersensor communication. However, intersensor communication is performed after the distributed compression of sensor observations (as explained above), thereby reducing the amount of data exchange. Further, we assume that the DGN broadcasts the updated encoding information $i(k, j)$ of each sensor of a cluster once every T_e seconds. (Hence, each node knows the encoding information of others within its own cluster.) At each node, the compressed data corresponding to all N_e samples within the entire period of T_e are concatenated into a single stream of $i(k, j)N_e$ bits. Local communication among cluster members is performed once every T_e seconds to exchange these compressed data streams corresponding to blocks of N_e samples. The transmission of data from a cluster to the DGN is known as long-haul communication [see Fig. 1(b)].

Let us assume that each node in a cluster transmits its data during the local communication step using M-ary QAM. The nodes share the wireless channel via time-division multiplexing. When the length of the bit stream $i(k, j)N_e$ is not divisible by $\log_2 M$, the M-QAM implementation may require N_d number of tail bits to be added to the data stream. At the end of the local communication step, the original data bits can be demodulated simply by removing the extra tail bits (this is possible since each node knows $i(k, j)$ values of others in its cluster). The proposed block-based local communication of once every T_e seconds reduces the extra energy needed to spend on tail bits. Also, it should be emphasized that the required intersensor communication is considerably reduced since local communication is performed only on compressed data.

At the end of the local communication step, each cluster node combines data symbols broadcasted by all the nodes in its cluster into a single stream. Once this is done, each node in a cluster acts as if it were an element of a centralized antenna array. Thus-formed virtual antenna array then space–time block encodes the cluster data sequence that is to be sent to the DGN. This assumes that the data streams at all antenna elements (sensor nodes) are the same. In practice, channel errors during local communication may result in unequal data streams at cluster members, which leads to error propagation. It is, however, reasonable to assume that a sufficiently small error rate can be ensured during local communication with judicious choice of system parameters since clusters have a small radius that leads to relatively small transmission power requirements. Let us denote the symbol stream of the jth node by $b_k^{(j)}$ and consider, for simplicity, a cluster consisting of only two nodes. At the end of local communication, two nodes in the cluster have following symbols at time k: 1) $b_k^{(1)}$ and $\hat{b}_k^{(2,1)}$ at node 1; and 2) $b_k^{(2)}$ and $\hat{b}_k^{(1,2)}$ at node 2, where $\hat{b}_k^{(j,j')}$ is the estimate of $b_k^{(j)}$ at node j'. The space–time block encoding (which, in this case, is the Alamouti scheme) is implemented as follows: At the first time instant, nodes 1 and 2 transmit $b_k^{(1)}$ and $b_k^{(2)}$, respectively. At the second time instant, nodes 1 and 2 transmit $-(\hat{b}_k^{(2,1)})^*$ and $(\hat{b}_k^{(1,2)})^*$, respectively.

Note that a cooperative source-channel coding scheme having essentially the same local and long-haul communication steps as above has previously been proposed in [26]. However, there are notable differences. First, Murugan *et al.* [26] assumed an AWGN channel. Thus, effectively, the MIMO (or cooperative) gain in [26] is achieved by using a (spatial) repetition code without having to use any elaborate space–time (block) code. Moreover, in [26], the distributed compression is achieved using punctured low-density parity check codes. The implementation requires that each node be able to turbo-decode the received data during local communications. This can, of course, lead to complex node design requirements, whereas the proposed approach does not require such decoders at distributed nodes.

III. Adaptive Signal-Processing-Aided Side Information Computation

A. RLS-Based Correlation Tracking Algorithm

Without loss of generality, let us assume that the sensors are labeled according to the order they are decoded at the DGN, starting with a reference sensor. In general, the DGN's prediction $Y_k^{(j)}$ of sensor reading $X_k^{(j)}$ is formed using a linear combination of M_1 past readings of the jth sensor, and current and M_2 past readings of already decoded sensors as follows:

$$Y_k^{(j)} = \sum_{l=1}^{j-1} \alpha_l^{(j)} X_k^{(l)} + \sum_{i=1}^{M_1} \beta_i^{(j)} X_{k-i}^{(j)} + \sum_{i=1}^{j-1} \sum_{l=1}^{M_2} \xi_{l,i}^{(j)} X_{k-l}^{(i)} \tag{1}$$

where $\alpha_l^{(j)}$, $\beta_i^{(j)}$, and $\xi_{l,i}^{(j)}$ are the weighting coefficients. Note that (1) is a generalization of the linear predictive model proposed in [3]. As we will discuss in Section V, the inclusion of past readings leads to improved performance both in terms of node energy efficiency and decoding error rates at the expense of increased computational complexity at the DGN.

In vector form, (1) can be written as $Y_k^{(j)} = \underline{\theta}^{(j)T} \underline{z}^{(j)}(k)$, where, with $M_2 = 0$ for brevity, $\underline{\theta}^{(j)} = (\alpha_1^{(j)}, \alpha_2^{(j)}, \ldots, \alpha_{j-1}^{(j)}, \beta_1^{(j)}, \ldots, \beta_{M_1}^{(j)})^T$, $\underline{z}^{(j)}(k) = (X_k^{(1)}, X_k^{(2)}, \ldots, X_k^{(j-1)}, X_{k-1}^{(j)}, \ldots, X_{k-M_1}^{(j)})^T$, and the superscript ^{T} denotes the transpose of a vector or a matrix (note that the following vector equations apply to the general case with nonzero M_2). The prediction error is given by

$$e_k^{(j)} = X_k^{(j)} - Y_k^{(j)} = X_k^{(j)} - \underline{\theta}^{(j)T} \underline{z}^{(j)}(k). \tag{2}$$

In the previously proposed approaches to computing side information at the DGN, the prediction coefficient vector $\underline{\theta}^{(j)}$ was chosen to minimize the mean squared error (MSE) defined as $E[{e_k^{(j)}}^2]$ and adapted with the well-known least mean squares (LMS) algorithm [3]. On the other hand, in this paper, we propose to choose the filter coefficient vector $\underline{\theta}^{(j)}$ to minimize the weighted least-squares prediction error at time k defined as $J(k) = \sum_{n=0}^{k} \lambda^{k-n} |e_n^{(j)}|^2$, where $0 < \lambda < 1$ is the so-called *exponential forgetting factor*. Note that unlike the minimum MSE solution that is the same for all sequences of data having the same statistics, the least-squares solution that minimizes $J(k)$ depends explicitly on the particular realization of data.

Setting the derivative of $J(k)$ with respect to $\underline{\theta}^{(j)}(k)$ to zero gives the least squares solution

$$\underline{\theta}_{\text{opt}}^{(j)}(k) = (R^{(j)}(k))^{-1} \, \underline{r}_{zx}^{(j)}(k) \tag{3}$$

where $R^{(j)}(k) = \sum_{n=0}^{k} \lambda^{k-n} \underline{z}^{(j)}(n) \underline{z}^{(j)T}(n)$ is the exponentially weighed deterministic autocorrelation matrix of data, and $\underline{r}_{zx}^{(j)}(k) = \sum_{n=0}^{k} \lambda^{k-n} \underline{z}^{(j)}(n) X_n^{(j)}$ is the cross correlation between data $\underline{z}^{(j)}(n)$ and the desired output $X_n^{(j)}$.

In practice, $\underline{\theta}_{\text{opt}}^{(j)}(k)$ in (3) needs to be updated for each k. If at the kth time instant $\underline{\theta}^{(j)}(k) = (R^{(j)}(k))^{-1} \underline{r}_{zx}^{(j)}(k)$, then it can be shown that the recursive update of the coefficient vector at the $(k+1)$th time instant is

$$\underline{\theta}^{(j)}(k+1) = \underline{\theta}^{(j)}(k) + \underline{g}^{(j)}(k+1) e_{k+1}^{(j)} \tag{4}$$

where $\underline{g}^{(j)}(k+1)$ is the gain vector defined as

$$\underline{g}^{(j)}(k+1) = \frac{\lambda^{-1}(R^{(j)}(k))^{-1} \underline{z}^{(j)}(k+1)}{1 + \lambda^{-1} \underline{z}^{(j)T}(k+1)(R^{(j)}(k))^{-1} \underline{z}^{(j)}(k+1)}.$$

It is well known that a faster rate of convergence as well as a relatively smaller prediction error can be obtained with an RLS-based adaptive algorithm compared to that of an LMS-based approach. Thus, it can be argued that the proposed method is better suited for highly dynamic data environments requiring a faster rate of convergence than that offered by the LMS-based approach. In addition, the smaller prediction error leads to better energy efficiencies at the distributed nodes and smaller decoding errors at the DGN, as we will show in Section V.

B. Encoding Side-Information Computation

As mentioned earlier, if the actual reading $X_k^{(j)}$ and the prediction $Y_k^{(j)}$ are not more than $2^{i(k,j)-1}\Delta$ apart, then $X_k^{(j)}$ will be decoded correctly at the DGN. Assuming that the prediction error $e_k^{(j)}$ is distributed with a zero mean and a variance $\sigma^2_{e_k^{(j)}}$, Chou *et al.* [3] bounded the probability of decoding error as $P[|e_k^{(j)}| > 2^{i(k,j)-1}\Delta] \le \sigma^2_{e_k^{(j)}} / (2^{i(k,j)-1}\Delta)^2$ via the Chebyshev inequality. If the probability of decoding error is to be less than a given threshold P_e, then the required encoding side information is

$$i(k,j) = \frac{1}{2} \log_2 \left(\frac{\sigma^2_{e_k^{(j)}}}{\Delta^2 P_e} \right) + 1. \tag{5}$$

However, experiments with real sensor data show that, typically, it is reasonable to assume that the prediction error $e_k^{(j)}$ is Gaussian distributed. If we assume that $e_k^{(j)}$ is Gaussian with zero mean and a variance of $\sigma^2_{e_k^{(j)}}$, the probability of decoding error can then be approximated as $P_e = P(|e_k^{(j)}| > 2^{i(k,j)-1}\Delta) \approx 2Q(2^{i(k,j)-1}\Delta / \sigma_{e_k^{(j)}})$, where $Q(.)$ denotes the standard Gaussian tail distribution function. This leads to the following new expression for the encoding side information:

$$i(k,j) = \log_2 \left(\frac{\sigma_{e_k^{(j)}}}{\Delta} Q^{-1} \left(\frac{P_e}{2} \right) \right) + 1 \tag{6}$$

where $Q^{-1}(.)$ denotes the inverse Q-function. As we will confirm via experimental results in Section V, the Gaussian model based encoding side-information computation method seems to be efficient in most situations.

Computing $i(k,j)$ via either (5) or (6) requires knowledge of the prediction error variance $\sigma^2_{e_k^{(j)}}$ at the DGN. In order to initialize the correlation tracking algorithm, the DGN queries all sensors for their uncompressed readings for a training period of $N_{\rm tr}$ samples before starting real-time operation. At the end of this training period, the prediction error variance is initialized using the unbiased estimate $\sigma^2_{e_k^{(j)}} = (1/(N_{\rm tr}-1))\sum_{k=1}^{N_{\rm tr}} |e_k^{(j)}|^2$. In order to track the time-varying nature of the sensed data, this initial estimate is iteratively updated during real-time data compression using the filtered estimate

$$\sigma^2_{e_{k+1}^{(j)}} = (1-\gamma)\sigma^2_{e_k^{(j)}} + \gamma {e_k^{(j)}}^2$$

where $0 \leq \gamma \leq 1$ is a *forgetting factor* accounting for the effects of sudden (impulsive) variations in sensed data [33], and the prediction error $e_k^{(j)}$ is computed in decision-directed mode.

IV. Energy Analysis of the Integrated System

The two main components of power consumption along a signal path are due to that of power amplifiers and the circuit blocks of sensors, which are denoted, respectively, by $P_{\rm PA}$ and P_C [13], [14]. The amplifier power consumption term can be approximated as in [13] and [14] as

$$P_{\rm PA} = (1+\alpha)P_{\rm out} \tag{7}$$

where $\alpha = \xi/\eta - 1$, where η is the drain efficiency of the radio frequency power amplifier, and ξ is the peak-to-average ratio. If M-QAM is used, then $\xi = 3\left((M - 2\sqrt{M}+1)/(M-1)\right)$ [13]. The transmit power $P_{\rm out}$ can be determined as

$$P_{\rm out} = \frac{(4\pi)^2 d^\kappa M_l N_f}{G_t G_r \lambda^2}\bar{E}_b R_b \tag{8}$$

where d is the transmission distance, κ is the path loss exponent, G_t and G_r are the transmitter and receiver antenna gains, respectively, λ is the carrier wavelength, M_l is the link margin, N_f is the receiver noise figure, $\bar{E}_b$ is the average energy per bit required for a given bit error rate (BER) $\bar{P}_b$, and R_b is the system bit rate. The receiver noise figure N_f is given by $N_f = N_r/N_0$, where N_r is the power spectral density (PSD) of the total effective noise at the receiver input, and N_0 is the single-sided thermal noise PSD at room temperature.

The energy spent by a node can be computed in two steps: energy spent for local communication and that spent for long-haul communication. During local communications, the power consumed by the circuit blocks of a node in broadcasting its data can be approximated as $P_C^{(\rm Loc_{Tx})} \approx P_{\rm DAC} + P_{\rm mix} + P_{\rm filt} + P_{\rm synth}$, where $P_{\rm DAC}$, $P_{\rm mix}$, $P_{\rm filt}$, and $P_{\rm synth}$ are the power consumption values of the digital-to-analog converter, the mixer, the active filters at the transmitter side, and the frequency synthesizer, respectively. Similarly, the node circuit power consumption in receiving broadcasted data from other nodes in its cluster can be given by $P_C^{(\rm Loc_{Rx})} \approx P_{\rm synth} + P_{\rm LNA} + P_{\rm mix} + P_{\rm IFA} + P_{\rm filr} + P_{\rm ADC}$, where $P_{\rm LNA}$, $P_{\rm IFA}$, $P_{\rm filr}$, and $P_{\rm ADC}$ are the powers consumed by low noise amplifier (LNA), the intermediate frequency amplifier (IFA), the active filters at the receiver side, and the ADC, respectively.

Since local communication is over a very short distance, the local channel is assumed to be AWGN. Suppose further that we use M-QAM with $b = \log_2 M$. Then, for a fixed average BER of $\bar{P}_b$, we have

$$\bar{E}_b^{\rm Loc} = \frac{(M-1)N_o}{3b}\left[Q^{-1}\left(\frac{\bar{P}_b\, b}{4\left(1-\frac{1}{\sqrt{2^b}}\right)}\right)\right]^2 \tag{9}$$

if $b \geq 2$ and even. When b is odd, $\bar{E}_b^{\rm Loc}$ can be approximated by dropping the term $(1-(1/\sqrt{2^b}))$ in the denominator of the argument of inverse Q-function in (9) [14]. The power amplifier power consumption during local communication $P_{\rm PA}^{(\rm Loc)}$ is then computed from (7) and (8), where $\bar{E}_b$ and d are replaced with $\bar{E}_b^{\rm Loc}$ in (9) and the worst-case distance $d_{\rm Loc}$ between any pair of sensors within a cluster, respectively.

Let $R_b^{(\rm Loc)}$ denotes the bit rate for local communication. The total energy consumption per bit (at a node) for local communication in V-STBC can then be estimated as

$$E_t^{\rm Local} = \frac{P_{\rm PA}^{(\rm Loc)} + P_C^{(\rm Loc_{Tx})} + (N_s-1)\times P_C^{(\rm Loc_{Rx})}}{R_b^{(\rm Loc)}}. \tag{10}$$

As no energy constraints are assumed on the DGN, the total circuit energy consumption of a cluster during long-haul communication can be approximated as $P_C^{(\rm Long)} \approx (P_{\rm DAC} + P_{\rm mix} + P_{\rm filt} + P_{\rm synth}) \times N_s$. Let us denote the power amplifier energy consumption per cluster during long-haul communication by $P_{\rm PA}^{(\rm Long)}$. Again, $P_{\rm PA}^{(\rm Long)}$ can be computed from (7) and (8) by assuming that $\bar{E}_b = \bar{E}_b^L$ and $d = d_{\rm Long}$, where $\bar{E}_b^L$ is the per bit energy per cluster for long-haul communications, and $d_{\rm Long}$ is the distance between the cluster and the DGN. Note that it is the long-haul communication over a fading channel that benefits from the proposed V-MIMO communications. For a 2×1 Alamouti system, under the assumptions of a Rayleigh fading channel and BPSK modulation, $\bar{E}_b^L$ can be computed by inverting (throughout this paper, we assume that DGN has perfect knowledge of the channel fading coefficients)

$$\bar{P}_b = \frac{1}{4}\left(1 - \frac{1}{\sqrt{1+\frac{1}{\bar{E}_b^L}/2N_o}}\right)^2\left(2 + \frac{1}{\sqrt{1+\frac{1}{\bar{E}_b^L}/2N_o}}\right). \tag{11}$$

The BER of an M-ary QAM STBC-based $2\times N_R$ MIMO system ($M = 2^b$) with a square constellation (i.e., b is even) for $b \geq 2$ can be shown to be given by

$$\bar{P}_b = \frac{4}{b}\left(1-\frac{1}{2^{b/2}}\right)\frac{1}{2^{2N_R}}\left(1 - \frac{1}{\sqrt{1+\frac{1}{\bar{E}_b^L}/2N_o}}\right)^{2N_R} \times \sum_{k=0}^{2N_R-1}\frac{1}{2^k}\binom{2N_R-1+k}{k}\left(1+\frac{1}{\sqrt{2+\frac{1}{\bar{E}_b^L/2N_o}}}\right)^k. \tag{12}$$

When $b \geq 2$ is odd, we can use (12) as an upper bound for the BER after dropping the term $(1-(1/2^{b/2}))$. By (numerically) inverting (12), $\bar{E_b}^L$ can be computed for a fixed $\bar{P}_b$.

If we denote by $R_b{}^{(\text{Long})}$ the bit rate for long-haul communication, then the total energy consumption per bit for a cluster during long-haul communication can be approximated as

$$E_t^{\text{Long}} = \frac{P_{\text{PA}}{}^{(\text{Long})} + P_C^{(\text{Long})}}{R_b{}^{(\text{Long})}}. \tag{13}$$

To be complete, we need to take into account three additional energy terms that arise due to the following: 1) initial training; 2) reception of encoding information $i(k,j)$; and 3) extra tail bits. Recall that during the initial system training, each node accumulates N_{tr} samples and broadcasts them (uncompressed) to other nodes in its own cluster via local communication. Once every node has samples of all other nodes in its own cluster, the cluster sends all these samples to the DGN via distributed STBC. Thus, the total energy required for the initial training of all N_s nodes in a cluster is $E^{\text{Tr}} = (E_t^{\text{Local}} + E_t^{\text{Long}}) \times n \times N_s \times N_{\text{tr}}$, where n is the bits per sample at the output of ADCs.

In order to quantify the energy spent by distributed nodes in receiving encoding side information $i(k,j)$, let us assume that each node has a total of L data samples (including training samples) to be sent, and the bit rate of the feedback channel is also $R_b^{(\text{Long})}$. Since encoding side information is assumed to be updated once every N_e samples, the number of times the encoding side information is received by a node is $r = (L - N_{\text{tr}})/N_e$. Note that since $i(k,j) \leq n$, the encoding side information can be represented by using $\log_2(n)$ bits. Since each node receives all its fellow cluster members' encoding information, the total energy consumption by all nodes of a given cluster in receiving the encoding side information is $E^{\text{Re}} = r \times E_t^{\text{re}} \times \log_2(n) \times N_s^2$, where E_t^{re} is the reception energy per bit per node that can be given by $E_t^{\text{re}} = P_C^{(\text{Loc}_{\text{Rx}})}/R_b^{\text{Long}}$.

The number of tail bits added in mapping to M-ary QAM during local and long-haul communications is $N_d^{\text{local}} = \sum_{j=1}^{N_s}\sum_{p=0}^{r-1}[N_e i(pN_e+N_{\text{tr}}+1,j)] \bmod \log_2 M$ and $N_d^{\text{long}} = \sum_{p=0}^{r-1}([N_e \sum_{j=1}^{N_s} i(pN_e+N_{\text{tr}}+1,j)] \bmod \log_2 M)$, respectively. Hence, the total energy spent on tail bits in the case of V-STBC is $E^{\text{Extra}} = E_t^{\text{Local}} \times N_d^{\text{local}} + E_t^{\text{Long}} \times N_d^{\text{long}}$.

Thus, the total energy consumed by the proposed V-MIMO-based system in collecting L data samples from all N_s sensors of a cluster can be written as $E^{\text{Total}} = E^{\text{Comp}} + E^{\text{Tr}} + E^{\text{Re}} + E^{\text{Extra}}$, where E^{Comp} is the total energy spent in transmitting the compressed real-time data samples to the DGN given by

$$E^{\text{Comp}} = \left(E_t^{\text{Local}} + E_t^{\text{Long}}\right) \sum_{j=1}^{N_s} \sum_{k=N_{\text{tr}}+1}^{L} i(k,j). \tag{14}$$

In the following section, we characterize the energy efficiency of the proposed integrated system with respect to three reference systems. First is a single-input–single-output (SISO)-based system in which all nodes send their uncompressed readings to the DGN (i.e., SISO with no compression). The total energy consumption of this system is $E^{\text{Ref1}} = L \times E_t^{\text{SISO}} \times N_s \times (n + n \bmod \log_2 M)$, where E_t^{SISO} is the per-bit energy of a SISO system in Rayleigh fading. Note that E_t^{SISO} is computed using (7) and (13) as $E_t^{\text{SISO}} = (P_{\text{PA}}^{(\text{SISO})} + P_C^{(\text{Loc}_{\text{Tx}})})/R_b^{(\text{SISO})}$, where $R_b^{(\text{SISO})}$ is the bit rate of the SISO system. In this case, $P_{\text{PA}}^{(\text{SISO})}$ is computed as in (8) with $d = d_{\text{Long}}$ and $\bar{E}_b = (2(M-1)N_o/3b)\,((1 - (\bar{P}_b\, b/2(1-(1/\sqrt{2^b}))))^{-2} - 1)^{-1}$.

TABLE I

COMPARISON OF ENERGY SAVINGS FOR THE PROPOSED RLS-BASED ALGORITHM AND THE ALGORITHM IN [3] WITH ZERO DECODING ERRORS

Percentage of Energy savings	Humidity	Temperature	Light
Algorithm in [3]	30.37	43.48	11.01
Proposed Algorithm	45.23	60.20	21.25

In the second reference system, all nodes encode their readings using the proposed RLS-based distributed compression algorithm but employ SISO communication (i.e., SISO with compression). In this case, the overall energy consumption of the system is $E^{\text{Ref2}} = E^{\text{comp}} + E_t^{\text{SISO}} \times (N_{\text{tr}} \times n \times N_s + N_d^{\text{SISO}})$, where $E^{\text{comp}} = E_t^{\text{SISO}} \times \sum_{k=N_{\text{tr}}+1}^{L}\sum_{j=1}^{N_s} i(k,j)$, and $N_d^{\text{SISO}} = N_d^{\text{long}}$. Note that, here, we also assume that nodes send compressed readings to the DGN in blocks of N_e samples.

The third reference system uses virtual multiple-antenna clusters but no distributed source compression (i.e., V-MIMO without compression). The total energy consumption of this system is given by $E^{\text{Ref3}} = (E_t^{\text{Local}} + E_t^{\text{Long}}) \times N_s \times L \times (n + n \bmod \log_2 M)$.

The energy efficiency η_E of the integrated system with respect to any of the above reference schemes is defined as $\eta_E^{\text{Ref}} = \left((E^{\text{Ref}} - E^{\text{Total}})/E^{\text{Ref}}\right) \times 100\%$, where E^{Ref} can be either E^{Ref1}, E^{Ref2}, or E^{Ref3}.

V. PERFORMANCE RESULTS AND DISCUSSION

In this section, we first demonstrate the performance improvements obtained by the proposed RLS-aided distributed compression scheme compared to that of the LMS-aided method previously suggested in [3]. To be fair, we use exactly the same humidity, temperature, and light data sets that were used in [3]. In all cases, a 12-bit ADC is assumed so that $n = 12$. In case of humidity and temperature, the network had $N_s = 5$ nodes, while for light data, the network had $N_s = 4$ nodes. As can be observed from Table I, the proposed RLS-aided scheme offers an improvement of 10%–15% in energy savings compared to that of the algorithm in [3]. To be fair in comparisons, the encoding side information in these results was computed via (5), and $M_2 = 0$, as assumed in [3]. We further investigated the effect of nonzero M_2 on energy efficiency with both the proposed RLS-based approach and Chou *et al.*'s [3] LMS-based approach. Our results indicate that including a reasonably small number of past observations in the prediction model ($M_2 = 4$, for example) may improve the energy savings by an additional 5%–10%. This performance gain stems from the better correlation tracking achieved by the modified prediction model (1). For example, Fig. 2(a)

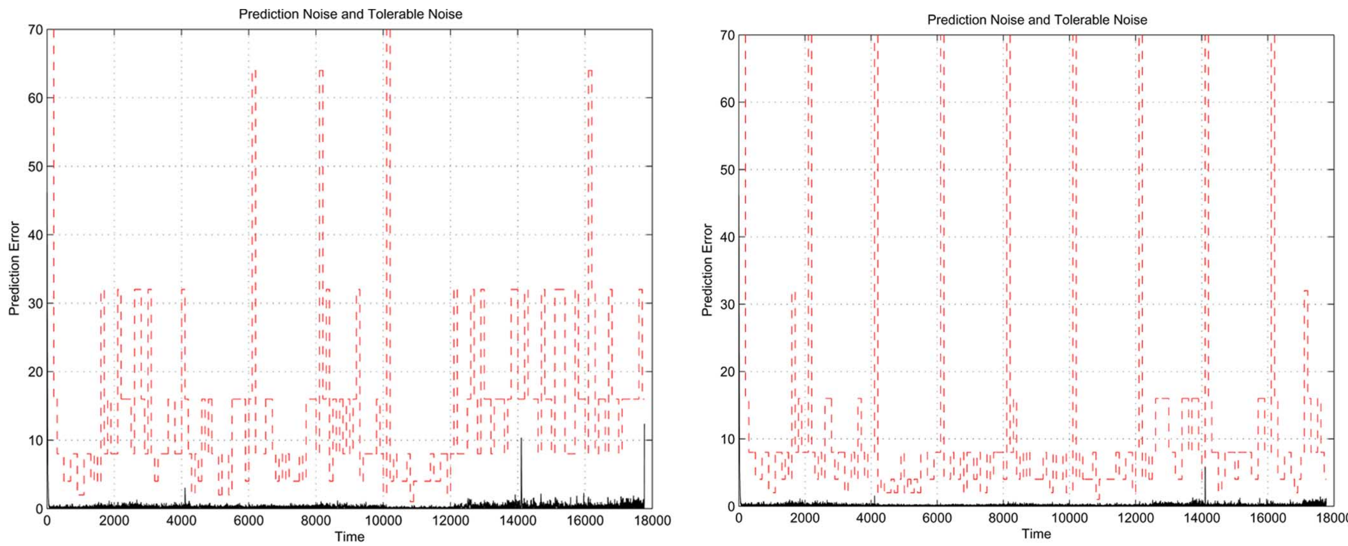

(a) (b)

Fig. 2. (Dotted line) Tolerable noise versus (solid line) actual prediction noise for humidity data set ($P_e = 0.001$, $\gamma = 0.5$, $\mu = 10^{-5}$, $T = 100$, and zero decoding errors). (a) Prediction model of Chou *et al.* [3] with $M_2 = 0$ (Energy Savings $= 30.37\%$). (b) Modified prediction model with $M_2 = 4$ (Energy Savings $= 35.48\%$).

and (b) shows the comparison between the actual prediction noise $e_k^{(j)}$ and the tolerable noise levels for humidity data with the prediction model of Chou *et al.* [3] and with the proposed modified prediction model, respectively. For the chosen parameters corresponding to Fig. 2(a) and (b), the maximum tolerable noise level is 128 (not shown in the graph for clarity). Apart from the prediction models used, both figures correspond to the LMS-based adaptive algorithm of Chou *et al.* [3]. Observe that the actual prediction error level in Fig. 2(b) is much smaller than that in Fig. 2(a). This shows the effectiveness of the modified linear prediction model. Moreover, as can be seen by comparing the two figures, the gap between tolerable noise and actual noise is narrower in Fig. 2(b) than that in Fig. 2(a), which indicates the better energy savings achieved by the proposed prediction model.

In Fig. 2(a) and (b), the gap between the actual prediction error and the tolerable noise is unnecessarily too large. This is wasteful and leads to less energy savings. The proposed least-squares approach leads to much better energy savings by considerably decreasing this wasteful margin of error, as seen in Fig. 3. Note that Fig. 3 corresponds to the same prediction model (and the humidity data set) as in Fig. 2(a) but uses the proposed RLS-based approach in place of the LMS-based approach of Chou *et al.* [3] assumed in Fig. 2(a). Comparison of Figs. 2(a) and 3 shows the improvement in energy efficiency with the proposed RLS-based algorithm, since it has significantly reduced the tolerable noise level while still keeping it above the actual noise level (which has also been reduced). As noted earlier, the performance of the RLS-based approach can further be improved by employing past data of other sensors (i.e., $M_2 \neq 0$) in the prediction model.

Next, we semi-analytically evaluate the energy efficiency of the integrated system with V-MIMO and distributed compression. For this, we again use the same humidity and temperature data sets that were used in [3] and assume that the nodes are organized as clusters. In particular, we choose four nodes and

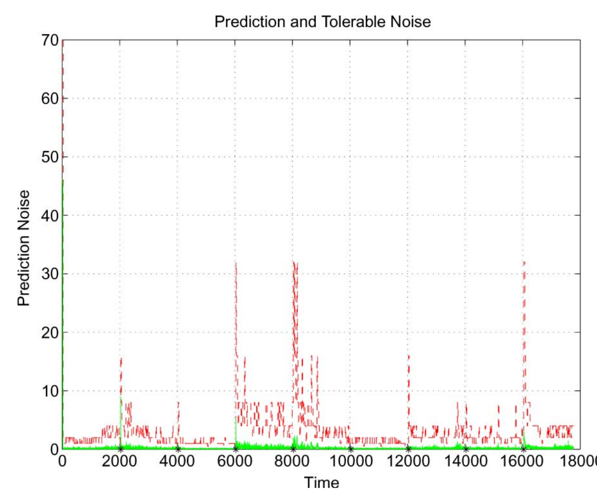

Fig. 3. (Dotted line) Tolerable noise versus (solid line) actual prediction noise of the proposed algorithm for humidity data with zero decoding errors (Energy Savings $= 45.23\%$).

assign them to two clusters. We assume a perfect feedback channel from the DGN to the sensor nodes and set $d_{\mathrm{Loc}} = 10$ m. (Note that clustering and the value of d_{Loc} are chosen arbitrarily.) Thus, our sensor network consists of two virtual antenna arrays (each having two elements) and a single DGN. The power consumption parameters are the same as that assumed in [13], i.e., $P_{\mathrm{mix}} = 30.3$ mW, $P_{\mathrm{filt}} = 2.5$ mW, $P_{\mathrm{filr}} = 2.5$ mW, $P_{\mathrm{LNA}} = 20$ mW, $P_{\mathrm{synth}} = 50$ mW, $M_l = 40$ dB, $N_f = 10$ dB, $G_t G_r = 5$ dBi, and $\eta = 0.35$. Additionally, in all the results, $N_{\mathrm{tr}} = 65$, $N_e = 20$, and the local communication is with 16-QAM. The encoding information is computed using (5) as in [3]. Fig. 4(a) shows the per-bit energy consumption of the proposed integrated V-MIMO-based scheme and that of the SISO-based (still with distributed compression) scheme with different M-QAM orders assuming a path loss exponent of $\kappa = 2$. Observe from Fig. 4(a) that for large-enough long-haul distances, there are considerable energy savings

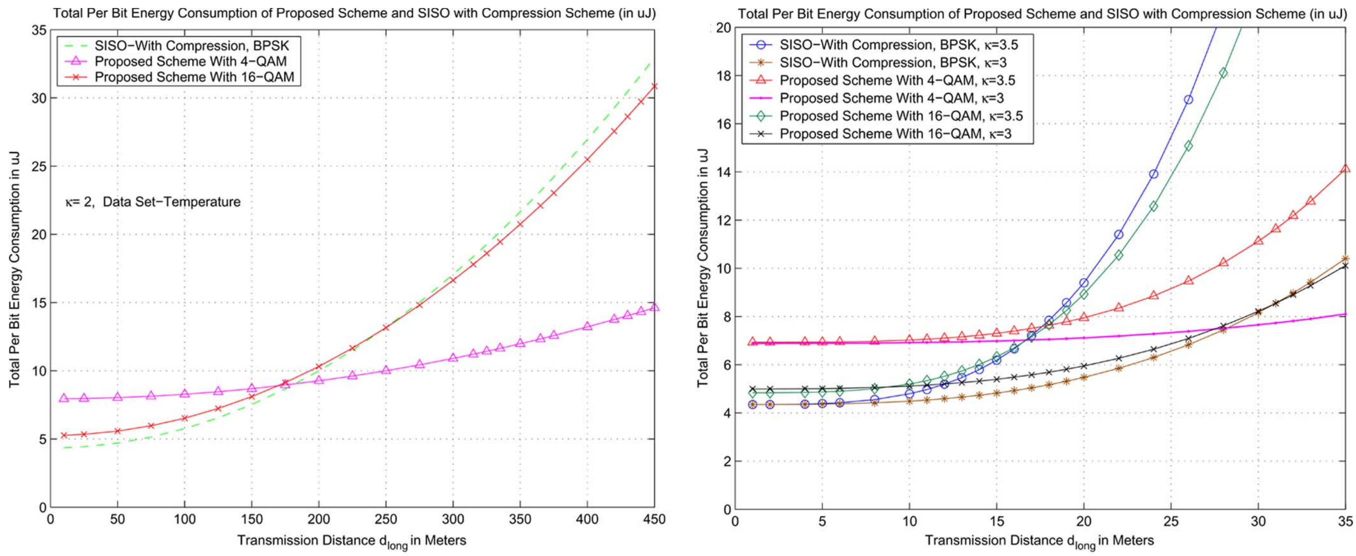

(a) (b)

Fig. 4. Comparison of the per-bit energy consumption of the proposed scheme (with both 4-QAM and 16-QAM) with that of BPSK-based SISO with compression scheme. (a) $\kappa = 2$. (b) $\kappa = 3$ and $\kappa = 3.5$.

to be achieved with the V-MIMO-based approach compared to that of SISO-based communication. Moreover, the region in which the V-MIMO-based scheme is inferior to that of the SISO-based scheme is considerably smaller than that in Fig. 4(a) for most realistic wireless path loss exponents. For example, most near-earth propagation channels usually have $3 \leq \kappa \leq 6$ [34]. With larger κ, the proposed integrated system based on V-MIMO outperforms the corresponding SISO-based systems even for relatively smaller d_{Long} distances, as shown in Fig. 4(b). For instance, when $\kappa \geq 3$, the proposed scheme with fixed 4-QAM provides enormous energy savings over the corresponding SISO-based system even for a few tens of meters of long-haul distance.

In situations where an increase in node and system design complexity can be tolerated, it has been suggested that rate optimization can be used to improve the performance of V-MIMO schemes [13], [14]. In this case, for each long-haul distance, we find the optimal M-QAM constellation size that results in the minimum per-bit energy. Fig. 5 shows the overall energy consumption per information bit for the proposed and three reference schemes defined earlier with rate-optimized M-QAM for long-haul communication (again, a 16-QAM system is assumed for local communication) assuming that $\kappa = 2$. It can be seen from Fig. 5 that the proposed integrated system outperforms SISO without compression scheme after about 25 m, and SISO with compression scheme after about 125 m. More importantly, however, for long-haul distances below 125 m, the performance of the proposed scheme now almost matches with that of the SISO-based compression scheme. Hence, the proposed scheme with rate optimization can be used without considerable loss in energy savings for $d_{\mathrm{Long}} < 125$ m but with significant savings for $d_{\mathrm{Long}} > 125$ m.

In Fig. 6, we have shown the performance gain due to the proposed new method (6) for computing the encoding information based on Gaussian error approximation. Fig. 6(a) and (b) shows the per-bit energy of a 2 × 2 V-MIMO-based

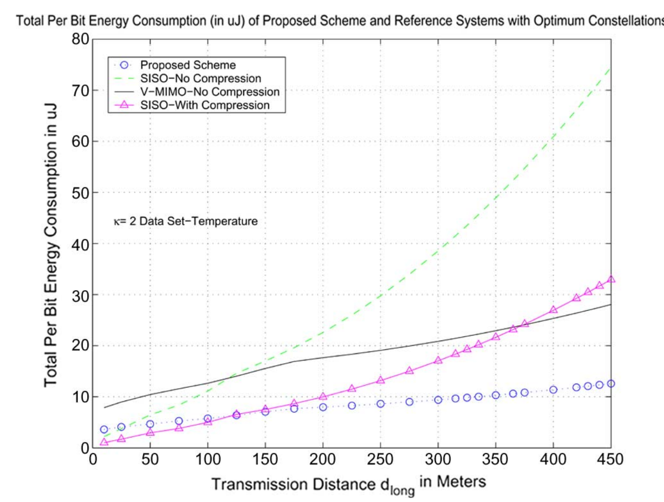

Fig. 5. Total per-bit energy consumption with optimal constellations.

system (two antennas at the DGN and two sensors per cluster) with $\kappa = 3$ using, respectively, (5) and (6) for computing the encoding information. Comparing Fig. 6(a) and (b), we observe that the proposed new method provides an improved performance over the Chebyshev-bound-based method of Chou *et al.* [3], and the performance gain is more prominent for larger long-haul distances.

Table II summarizes the energy efficiencies of the proposed V-MIMO-based system with respect to the three reference systems defined above. (Note that η_E^1, η_E^2, and η_E^3 represent the efficiencies with respect to first, second, and third reference systems, respectively.) Table II is based on 4-QAM long-haul communication and 2 × 2 V-MIMO.

In the above results, we have assumed that all nodes in a cluster act as a single antenna array. Of course, this need not be the case. In particular, in a large sensor network, we may have clusters with a large number of nodes. In such situations,

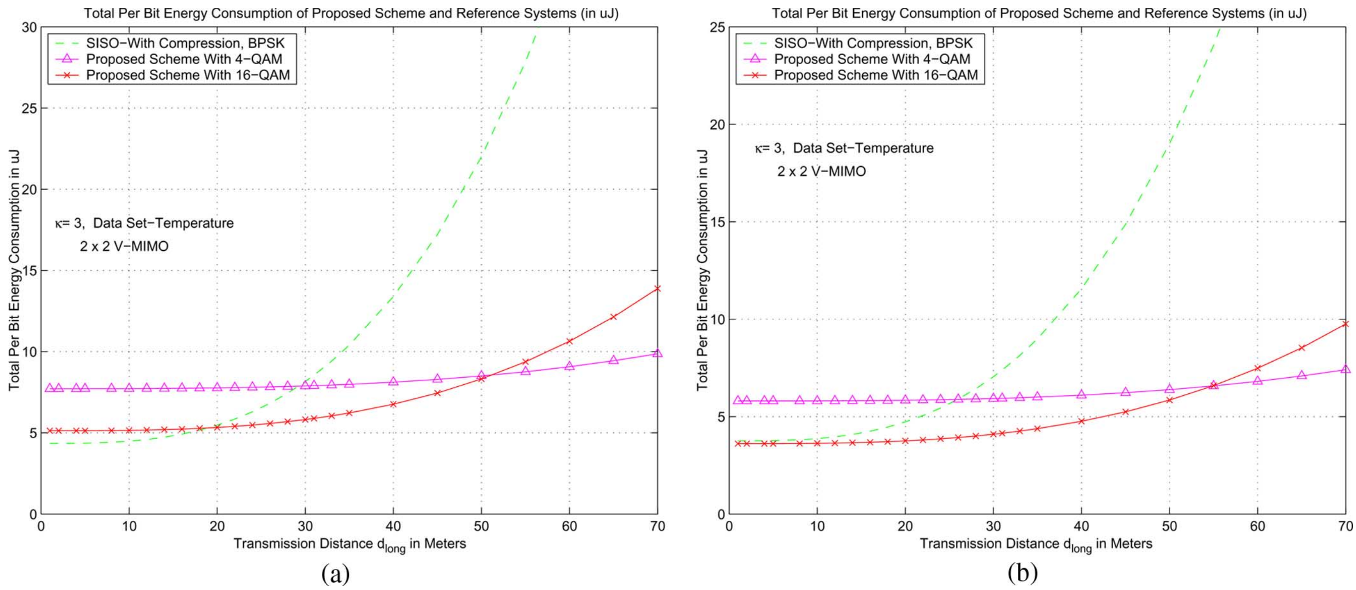

Fig. 6. Comparison of the per-bit energy consumption of the proposed scheme (with both 4-QAM and 16-QAM) with that of BPSK-based SISO with compression scheme. $\kappa = 3$. (a) Encoding information is computed via bounding the decoding error with Chebyshev's inequality. (b) Encoding information is computed by assuming that the prediction error is Gaussian.

TABLE II
ENERGY EFFICIENCIES (IN PERCENT) OF THE PROPOSED SCHEME WITH RESPECT TO DIFFERENT REFERENCE SYSTEMS
(2×2 V-MIMO, FIXED-RATE 4-QAM, $\kappa = 3$, GAUSSIAN PREDICTION ERROR APPROXIMATION)

d (m)	20	24	28	31	35	40	50	60	70
${\eta_E}^1$	40.89	56.52	68.15	74.61	80.95	86.33	92.26	95.09	96.59
${\eta_E}^2$	-51.03	-11.81	17.69	34.23	50.54	64.41	79.79	87.19	91.11
${\eta_E}^3$	61.70	61.71	61.72	61.73	61.74	61.76	61.81	61.89	61.97

we may have several virtual antenna arrays within a single cluster. Moreover, the distributed compression does not have to be necessarily with respect to the nodes inside a single cluster. If two clusters are close enough, there may be a considerable amount of spatial correlations among them that we may want to exploit. As an example, in Fig. 7, we have shown the topology of a larger WSN that was built at the Advanced Wireless Sensors Research Lab (AWSRL) at Wichita State University. This sensor network consists of 12 Crossbow MicaZ motes and a single DGN. The network has three clusters with four sensors per each cluster. Within each cluster, nodes are again separated into two pairs forming two virtual antenna arrays. The sensors within each cluster were closely located compared to the distance between two clusters (typically 4 and 12 m, respectively). A total of 4115 temperature data samples per sensor were collected during two consecutive days, and an intermediate system training is allowed during the transition from day-1 samples to day-2 samples.

Fig. 8(a) and (b) shows the per-bit energy consumption against the long-haul transmission distance. Note that the path loss exponent is assumed to be $\kappa = 3$. We can see that the proposed V-MIMO-based integrated system outperforms the reference systems for realistic long-haul distances. Comparing Fig. 8(a) and (b), it can be observed that the performance gap between that of the proposed scheme and the V-MIMO with no compression scheme has reduced in the case of 4-QAM compared to BPSK. Thus, V-MIMO with higher-order modulation schemes may even be used as a tradeoff for distributed compression.

VI. CONCLUSION AND FUTURE WORK

We have proposed an integrated WSN design that combines the power of V-MIMO and signal-processing-aided distributed compression. We proposed an improved distributed compression scheme with side information based on RLS adaptivity and a modified linear prediction model for side-information computation. A new model for computing the encoding side information was also proposed. This improved distributed compression scheme was then integrated with V-MIMO-based communication. The nodes were arranged into clusters that formed virtual antenna arrays. An efficient implementation was obtained by sharing only the compressed data among cluster members and scheduling the communication in blocks of samples. It can be concluded from the numerical results that the proposed V-MIMO-based integrated system with distributed compression leads to significant energy savings compared to that of corresponding SISO-based systems for transmission distances

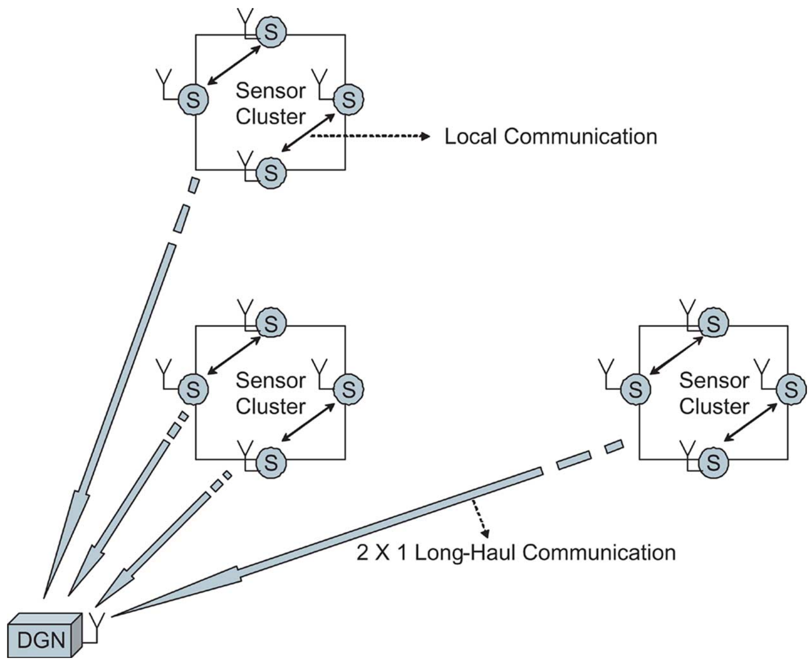

Fig. 7. Topology of the sensor network used for real-time temperature data collection at AWSRL.

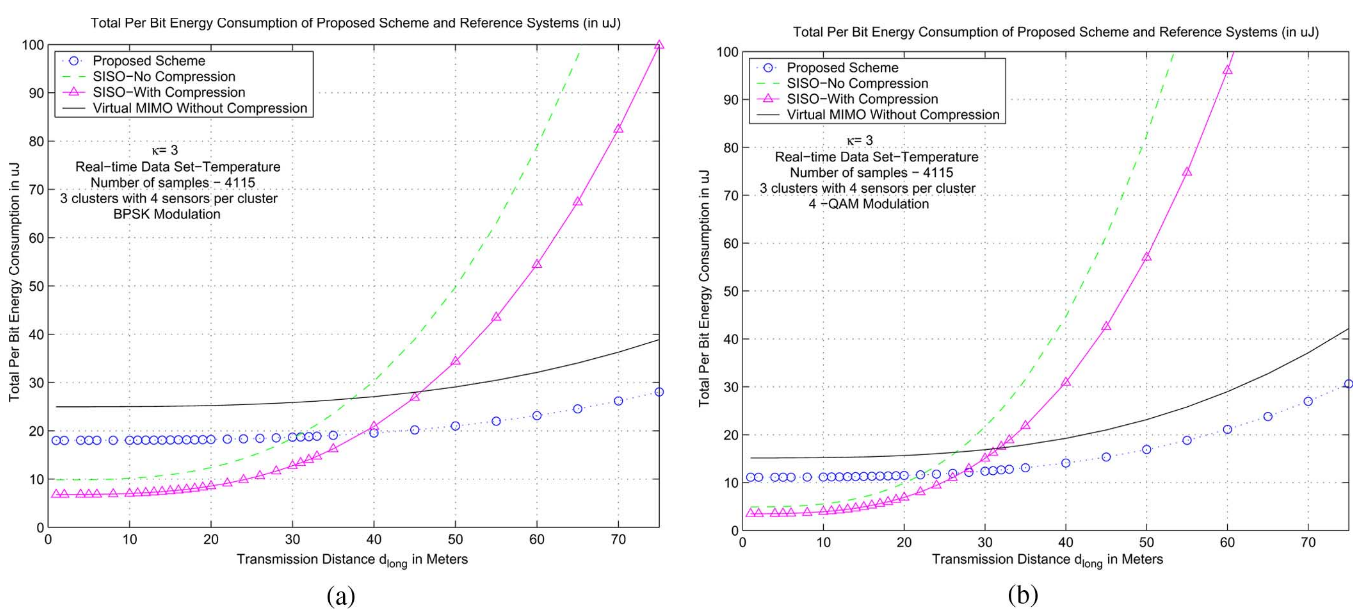

Fig. 8. Comparison of the per-bit energy consumption of the proposed scheme with that of the reference systems. $\kappa = 3$. (a) BPSK. (b) 4-QAM.

of a few tens of meters in realistic environments. Moreover, such significant system efficiencies can be made possible even with fixed modulation schemes.

Throughout this paper, we have assumed that the DGN has perfect channel state information and that the system is perfectly synchronous, both of which may not be true in practice. Efficient methods for channel estimation and synchronization that are suitable for V-MIMO-based wireless sensor systems as well as performance evaluation in the presence of estimation and synchronization errors are thus issues to be addressed in the future. Moreover, it is also possible to consider other V-MIMO and virtual antenna array [35] communication techniques in place of distributed STBC, as assumed in this paper. It is conceivable that certain MIMO techniques may lead to better integration efficiencies than others.

REFERENCES

[1] A. J. Goldsmith and S. B. Wicker, "Design challenges for energy-constrained *ad-hoc* wireless networks," *IEEE Trans. Wireless Commun.*, vol. 9, no. 4, pp. 8–27, Aug. 2002.

[2] M. Chu, H. Haussecker, and F. Zhao, "Scalable information-driven sensor querying and routing for *ad hoc* heterogeneous sensor networks," *Int. J. High Perform. Comput. Appl.*, vol. 16, no. 3, pp. 293–313, Fall 2002.

[3] J. Chou, D. Petrovic, and K. Ramchandran, "A distributed and adaptive signal processing approach to reducing energy consumption in sensor networks," in *Proc. IEEE INFOCOM*, San Francisco, CA, Mar. 2003, pp. 1054–1062.

[4] G. J. Foschini and M. J. Gans, "On limits of wireless communications in a fading environment when using multiple antennas," *Wirel. Pers. Commun.*, vol. 6, no. 3, pp. 311–335, Mar. 1998.

[5] I. E. Telatar, "Capacity of multi-antenna Gaussian channels," *Eur. Trans. Telecommun.*, vol. 10, no. 6, pp. 585–595, Nov. 1999.

[6] S. K. Jayaweera and H. V. Poor, "Capacity of multi-antenna systems with both receiver and transmitter channel state information," *IEEE Trans. Inf. Theory*, vol. 49, no. 10, pp. 2697–2709, Oct. 2003.

[7] H. Bolcskei and A. J. Paulraj, *Communications Hand Book*. Boca Raton, FL: CRC Press, 2002, pp. 90.1–90.14. ch. Multiple-input multiple-output (MIMO) wireless systems.

[8] R. Calderbank, A. Goldsmith, A. Paulraj, H. V. Poor, and E. Biglieri Eds., *MIMO Wireless Communication*. Cambridge, U.K.: Cambridge Univ. Press, 2007, to be published.

[9] S. M. Alamouti, "A simple transmit diversity technique for wireless communications," *IEEE J. Sel. Areas Commun.*, vol. 16, no. 8, pp. 1451–1458, Oct. 1998.

[10] V. Tarokh, H. Jafarkhani, and A. R. Calderbank, "Space–time block codes from orthogonal designs," *IEEE Trans. Inf. Theory*, vol. 45, no. 5, pp. 1456–1467, Jul. 1999.

[11] V. Tarokh, N. Seshadri, and A. R. Calderbank, "Space–time codes for high rate wireless communication: Performance criterion and code construction," *IEEE Trans. Inf. Theory*, vol. 44, no. 2, pp. 744–765, Mar. 1998.

[12] G. J. Foschini, "Layered space–time architecture for wireless communication in a flat fading environment when using multi-element antennas," *Bell Lab. Tech. J.*, vol. 1, no. 2, pp. 41–59, Autumn 1996.

[13] S. Cui, A. J. Goldsmith, and A. Bahai, "Energy-efficiency of MIMO and cooperative MIMO techniques in sensor networks," *IEEE J. Sel. Areas Commun.*, vol. 22, no. 6, pp. 1089–1098, Oct. 2004.

[14] S. K. Jayaweera, "Virtual MIMO-based cooperative communication for energy-constrained wireless sensor networks," *IEEE Trans. Wireless Commun.*, vol. 5, no. 5, pp. 984–989, May 2006.

[15] A. Sendonaris, E. Erkip, and B. Aazhang, "Increasing uplink capacity via user cooperation diversity," in *Proc. IEEE Int. Symp. Inf. Theory*, Cambridge, MA, Aug. 1998, p. 156.

[16] A. Sendonaris, E. Erkip, and B. Aazhang, "User cooperation diversity—Part I: System description," *IEEE Trans. Commun.*, vol. 51, no. 11, pp. 1927–1938, Nov. 2003.

[17] A. Sendonaris, E. Erkip, and B. Aazhang, "User cooperation diversity—Part II: Implementation aspects and performance analysis," *IEEE Trans. Commun.*, vol. 51, no. 11, pp. 1939–1948, Nov. 2003.

[18] J. Laneman and G. Wornell, "Exploiting distributed spatial diversity in wireless networks," in *Proc. 38th Allerton Conf. Commun., Control, Comput.*, Monticello, IL, Oct. 2000, pp. 1–10.

[19] J. N. Laneman, D. N. C. Tse, and G. W. Wornell, "Cooperative diversity in wireless networks: Efficient protocols and outage behavior," *IEEE Trans. Inf. Theory*, vol. 50, no. 12, pp. 3062–3080, Dec. 2004.

[20] A. Host-Madsen, "Capacity bounds for cooperative diversity," *IEEE Trans. Inf. Theory*, vol. 52, no. 4, pp. 1522–1544, Apr. 2006.

[21] A. Stefanov and E. Erkip, "Cooperative information transmission in wireless networks," in *Proc. Asian-Eur. ITW*, Breisach, Germany, Jun. 2002, pp. 90–93.

[22] M. C. Valenti and B. Zhao, "Capacity approaching distributed turbo codes for the relay channel," in *Proc. 57th IEEE VTC—Spring*, Jeju, Korea, Apr. 2003.

[23] S. Wei, D. L. Goeckel, and M. C. Valenti, "Asynchronous cooperative diversity," *IEEE Trans. Wireless Commun.*, vol. 5, no. 6, pp. 1547–1557, Jun. 2006.

[24] J. Laneman and G. Wornell, "Distributed space–time-coded protocols for exploiting cooperative diversity in wireless networks," *IEEE Trans. Inf. Theory*, vol. 49, no. 10, pp. 2415–2425, Oct. 2003.

[25] G. Scutari and S. Barbarossa, "Distributed space–time coding for regenerative relay networks," *IEEE Trans. Wireless Commun.*, vol. 4, no. 5, pp. 2387–2399, Sep. 2005.

[26] A. D. Murugan, P. K. Gopala, and H. E. Gamal, "Correlated sources over wireless channels: Cooperative source-channel coding," *IEEE J. Sel. Areas Commun.*, vol. 22, no. 6, pp. 988–998, Aug. 2004.

[27] G. Kramer, M. Gastpar, and P. Gupta, "Cooperative strategies and capacity theorems for relay networks," *IEEE Trans. Inf. Theory*, vol. 51, no. 9, pp. 3037–3063, Sep. 2005.

[28] M. Gastpar and M. Vetterli, "On the capacity of large Gaussian relay networks," *IEEE Trans. Inf. Theory*, vol. 51, no. 3, pp. 765–779, Mar. 2005.

[29] A. Host-Madsen and J. Zhang, "Capacity bounds and power allocation for wireless relay channels," *IEEE Trans. Inf. Theory*, vol. 51, no. 6, pp. 2020–2040, Jun. 2005.

[30] D. Slepian and J. K. Wolf, "Noiseless encoding of correlated information sources," *IEEE Trans. Inf. Theory*, vol. IT-19, no. 4, pp. 471–480, Jul. 1973.

[31] S. K. Jayaweera, "Energy efficient virtual MIMO-based cooperative communications for wireless sensor networks," in *Proc. 2nd ICISIP*, Chennai, India, Jan. 2005, pp. 1–6.

[32] S. K. Jayaweera, "An energy-efficient virtual MIMO communications architecture based on V-BLAST processing for distributed wireless sensor networks," in *Proc. 1st IEEE Int. Conf. SECON*, Santa Clara, CA, Oct. 2004, pp. 299–308.

[33] S. Haykin, *Adaptive Filter Theory*. Upper Saddle River, NJ: Prentice-Hall, 1996.

[34] G. L. Stüber, *Principles of Mobile Communication*. Norwell, MA: Kluwer, 1996.

[35] M. Dohler, E. Lefranc, and H. Aghvami, "Space–time block codes for virtual antenna arrays," in *Proc. PIMRC*, Lisbon, Portugal, Sep. 2002, pp. 414–417.

Sudharman K. Jayaweera (S'01–M'03) received the B.E. degree (with First Class Honors) in electrical and electronic engineering from the University of Melbourne, Melbourne, Vic., Australia, in 1997 and the M.A. and Ph.D. degrees in electrical engineering from Princeton University, Princeton, NJ, in 2001 and 2003, respectively.

From 1998 to August 1999, he was with the U.S. Wireless Corporation, San Ramon, CA, as a member of the Wireless Signal Processing Algorithms Development Group, where he was involved in developing wireless geolocation and tracking algorithms. From 2003 to 2006, he was an Assistant Professor in electrical engineering with the Department of Electrical and Computer Engineering, Wichita State University, Wichita, KS. He is currently an Assistant Professor in electrical engineering with the Department of Electrical and Computer Engineering, University of New Mexico, Albuquerque. His research interests include wireless communications, statistical signal processing, information theory, and wireless sensor networks.

Dr. Jayaweera currently serves as the Associate Editor of EURASIP *Journal of Applied Signal Processing*.

Madhavi L. Chebolu received the B.E. degree (with First Class Honors) in electronics and telecommunications engineering from Jawaharlal Technological University, Hyderabad, India, in 2001 and M.S. degree in electrical and computer engineering from Wichita State University, Wichita, KS, in 2005.

From 2002 to 2003, she was a Lecturer with the Electronics and Communications Engineering Department, Godavari Institute of Engineering and Technology, Rajahmundry, India. She is currently a Network Engineer with AT&T, Middletown, NJ. Her current research interests include wireless communications, wireless sensor networks, and computer networking.

Rakesh K. Donapati received the B.E. degree (First Class, with Distinction) in electronics and communications engineering from the University of Madras, Chennai, India, in 2004 and M.S. degree in electrical engineering from Wichita State University, Wichita, KS, in 2006.

He is currently a member of the Radio Test Set (RTS) Development Group with Aeroflex Test Solutions, Wichita, where he is involved in the development of hand-held communications and digital radio test sets. His research interests are in the areas of wireless communications, signal processing, and wireless sensor networks.